APEM journal
Advances in Production Engineering & Management
Volume 10 | Number 3 | September 2015 | pp 115–124
http://dx.doi.org/10.14743/apem2015.3.196
ISSN 1854-6250
Journal home: apem-journal.org
Original scientific paper

Characterizations of 304 stainless steel laser cladded with titanium carbide particles

Mahmoud, E.R.I.[a,*]

[a]Welding and NDT Laboratory, Manufacturing Technology Department, Central Metallurgical Research and Development Institute (CMRDI), Cairo, Egypt

ABSTRACT

The aim of this paper was to increase the wear resistance of the 304 stainless steel alloy without significant losses of its corrosion resistance. The YAG fiber laser was used to clad it with TiC powder at a fixed processing power of 2800 W and travelling speeds of 4 mm/s, 8 mm/s, and 12 mm/s. The TiC powder with a particle sizes of 3-10 μm were preplaced on a cleaned surface to form a layer of two different thicknesses: 1 mm and 2 mm. The shielding gas that used during and after laser cladding was argon with a flow rate of 15 l/min. Some of the TiC particles were melted and re-solidified as dendrites during the cladding processing. The amount of the dendritic TiC structure was increased by increasing of the travelling speed, and the cohesion of the cladding layer with the substrate was improved for the same reason. At lower travelling speed, cracks were appeared at both the interface and the heat affected zone. The TiC particles were clustered within the top portion of the cladding layer when the preplaced powder was 2 mm. The surface hardness and wear resistance were remarkably improved under all processing conditions, especially at higher travelling speeds. Moreover, the sample treated at a travelling speed of 12 mm/s showed better corrosion resistance than the stainless steel substrate.

ARTICLE INFO

Keywords:
Laser cladding
304 stainless steel alloy
TiC particles
Microhardness
Wear and corrosion resistance

**Corresponding author:*
emahoud@kku.edu.sa
(Mahmoud, E.R.I.)

Article history:
Received 30 December 2014
Revised 19 August 2015
Accepted 24 August 2015

1. Introduction

AISI 304 stainless steel alloy is widely used in many fields, such as oil, nuclear and chemical industries due to its specific properties, i.e. excellent corrosion resistance, good mechanical properties and accepted machinability [1-3]. This type of stainless steels is used as a structural material in hydraulic machinery and in liquid-handling systems [4, 5]. However, at severe environments, where the wear and cavitation attack are the main failure modes, this type of steel cannot be used due to its low surface hardness and wear resistance. Due to the contact between the components and a flowing or vibrating liquid, cavitation erosion represents a common type of degradation of components [6]. Generally, good wear, corrosion and oxidation resistances of different materials can be obtained by tailoring their surface properties. This can be done by depositing some alloys and/or ceramic powders on the material surfaces aiming to produce metal matrix composites (MMCs) on the treated surfaces. This can be produced by laser cladding. The advantages of this technique over the conventional ones (such as arc welding and thermal spraying) include: better coatings with dense microstructure, high wear resistance, low dilution and good metallurgical bonding to substrate [7-9]. Different substrate materials such as steels, aluminum [10, 11] and titanium alloys [12, 13] were cladded by this treatment. Ceramic

powders such as SiC [7], TiC [12, 13], and WC [14] without/or with some materials such as Ni-based alloy [15] were added as cladding materials. TiC is considered a good candidate in this field. This is due to its high thermal stability and high melting point, excellent wear resistance, low coefficient of friction, good resistance to thermal shock, high electrical and thermal conductivities [16]. For these reasons, it is widely used as reinforcement materials in many applications [17-19]. Moreover, the TiC particles have good compatibility with the iron base matrix [20].

Some works have been done to clad the stainless steel alloys with ceramic powder by using laser technique aiming to improve the wear and cavitation erosion resistances [21]. They add hard WC particles to increase the surface hardness which will increase the cavitation erosion resistance [22]. However, these hard WC particles damage the passive film, which is the first defense against any corrosive media [21]. In other studies, the surface hardening of austenitic stainless steel has been achieved by incorporating the hard particles of TiC, SiC, WC and alloying elements [23] in order to form carbides, nitrides [24] and borides [25]. In other studies, element such as Mo [26] was added to improve the pitting and intergranular corrosion resistance and to prevent stress corrosion cracking in acoustic environment. To widen the applications of 304 stainless steel alloy, it is important to improve its wear resistance without losses in its corrosion resistance. In the present study, 304 stainless steel substrate is laser cladded with TiC powder using YAG fiber laser. The effect of travelling speed and the thickness of the preplaced powder on the microstructural features, hardness, wear and corrosion resistance will be studied.

2. Experimental work

Stainless steel (304) specimens with dimensions of 100 mm × 50 mm × 3 mm were used as substrate materials. The specimens were ground using emery papers and cleaned in acetone to remove any dirt, oil, grease and other contaminants before treatment. The TiC powder with a particle size of 3-10 μm were preplaced on the cleaned surface to form a layer of two different thicknesses: 1 mm and 2 mm. The cladding treatments were carried out using YAG fiber laser of 3 kW. To avoid the oxidation during the treatment, argon gas with the flow rate of 15 l/min was used as a shielding gas. The treatments were carried out at fixed processing power of 2800 W, which was considered the optimum power during the preliminary experiments. Three different travelling speeds of 4 mm/s, 8 mm/s, and 12 mm/s were used in this study. The process was conducted at a defocusing distance (D_f) of 65 mm. The laser processed samples were analyzed as described in our work El-Labban et al. [27]. The microstructures of the coated layers were investigated using optical microscope and scanning electron microscope equipped with EDX analyzer. The micro-Vickers hardness in the coated layer cross-section and the substrate were measured with an indentation load of 9.8 N and loading time of 15 s at room temperature. The wear behaviour of the laser cladded zone was evaluated using a pin-on-disk dry sliding wear tester. A stationary sample with a diameter of 2.5 mm was slid against a rotating disk with a rotational speed of 265 rpm for 15 min. The tests were carried out at a fixed load of 2 kg applied to the pin. The differences in average weight before and after the wear test were measured and accounted. Three specimens of each condition were chosen for wear tests. The untreated base metal was selected as the reference material for the wear test. The corrosion behavior of the substrate and the cladding layer were evaluated by the corrosion current density and the corrosion potential obtained from polarization curves in a 3.5 wt.% NaCl solution at room temperature with an IM-6 electrochemical workstation. The scanning potential can be in the range of –1.0 V to +2 V, and the scanning rate was 5 mV/s [27].

3. Results and discussion

3.1 Microstructure analysis

The basic microstructure of the substrate, as shown in Fig. 1, is constituted of equiaxed, twinned austenitic-grain structure, which is the typical microstructure of the 304 austenitic stainless steel alloy. Macro-view of the cross-section of the cladding layer synthesized with laser power

and travelling speed of 2800 W and 12 mm/s, respectively is shown in Fig. 2. The cladding zone appeared as a concaved shape inside the base metal. The used large positive defocusing distance (65 mm) focus the heat into deeper areas, results in this concaved shape. Three zones were appeared in the cross-section of the laser treated area: TiC rich zone, heat affected zone and the substrate, as illustrated in Fig. 2

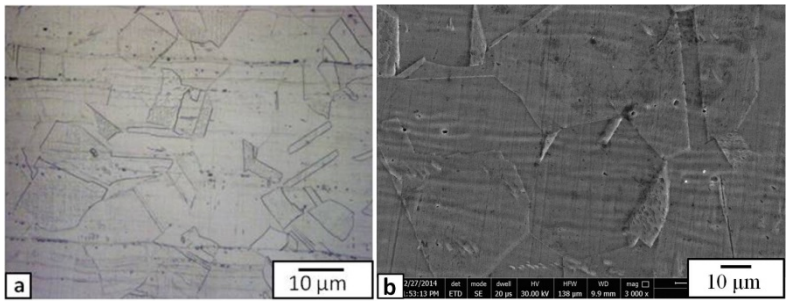

Fig. 1 Microstructure of the 304 stainless steel substrate

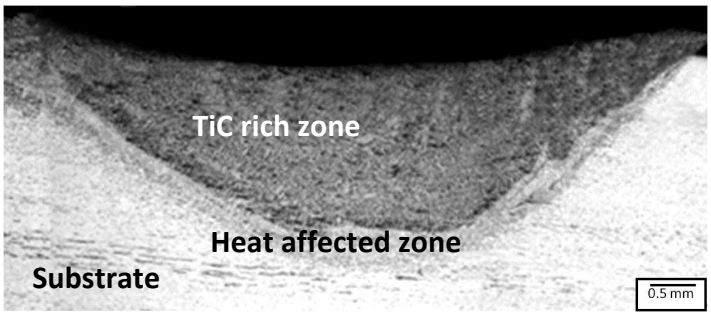

Fig. 2 Macrograph of the laser treated zone at power of 2800 W and travelling speed of 12 mm/s

Fig. 3 and Fig. 4 show the microstructures of the cladded layer fabricated with preplaced TiC powder of 1 mm thick and 4 mm/s travelling speed. Most of the TiC powder were dissolute in the matrix, forming fine dendrites with small arms as shown in Fig. 3(a) and Fig. 3(b). At the lower portion of the cladding layer, many cracks and crack networks were observed which starts from the interface and going upward into the cladding layer as shown in Fig. 3(c) and Fig. 3(d). This is may be due to the lower thermal conductivity of the stainless steel substrate, which may result in keeping of higher temperature for a longer time and reducing the cooling rate, and leads to formation of carbides at the grain boundary of the stainless steel side. This explanation was confirmed with the micrographs shown in Fig. 4. The treated specimen with this slow travelling speed of 4 mm/s had a wide heat affected zone, Fig. 4(a), and their grain boundaries were attacked, Fig. 4(b), due to the formation of carbides at the grain boundaries.

When the travelling speed was increased twice to be 8 mm/s, no micro-cracks were observed in the cladding layer or at the interface as shown in Fig. 5. The cladding layer looks adhered to the substrate and free from the macro-defects. The TiC particles were partially dissolute and appeared as fine long dendrites together with their original shape, especially at the top portion (near the free surface). At the lower portion (near the substrate), the TiC dendrites were shorter and they had random orientation, Fig. 5(b). This is mainly due to the lower heat dissipation to the lower thermal conductivity stainless steel substrate. Moreover, some pores were detected in the cladding layer.

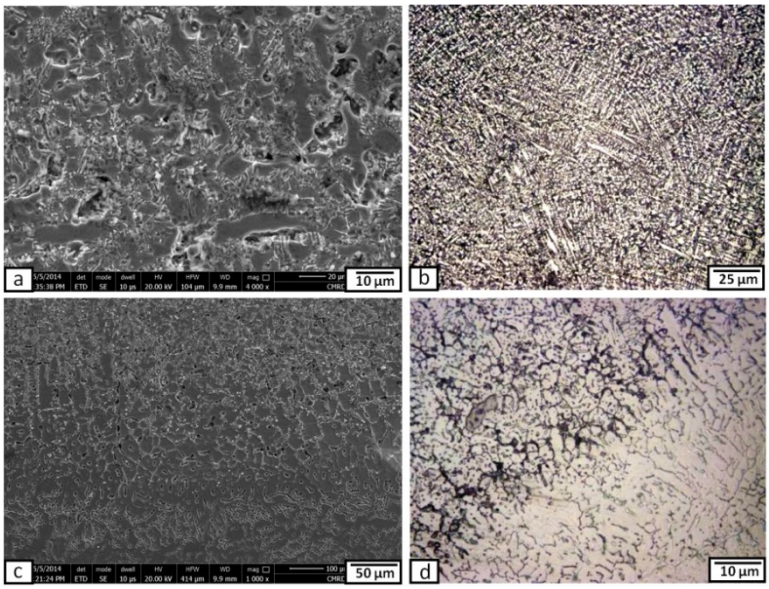

Fig. 3 Micrographs of the different zone at laser treated layer with power of 2800 W and travelling speed of 4 mm/s, when the thickness of preplaced TiC power was 1 mm, where (a) and (b) at the cladding layer, and (c) and (d) at the interface

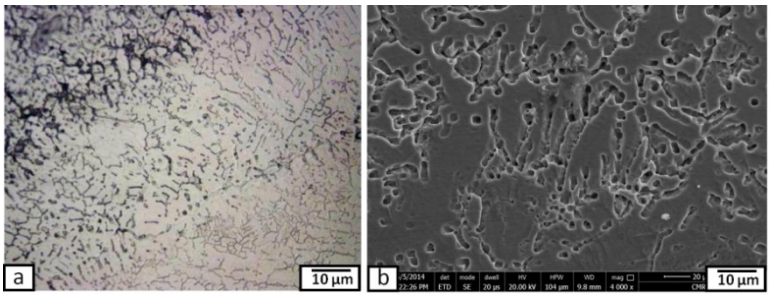

Fig. 4 Micrographs of the heat affected zone of the specimen treated with power of 2800 W and travelling speed of 4 mm/s, when the thickness of preplaced TiC power was 1 mm

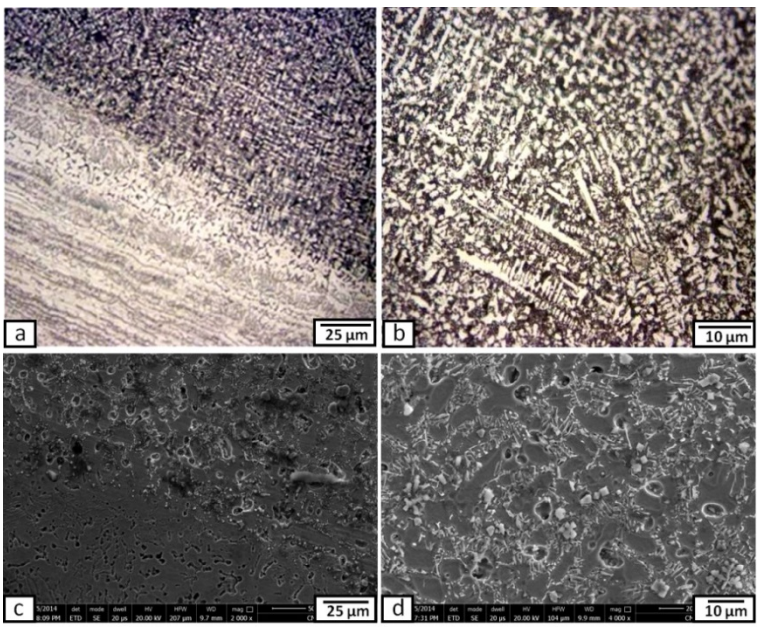

Fig. 5 Micrographs of the different zone at laser treated layer with power of 2800 W and travelling speed of 8 mm/s, when the thickness of preplaced TiC power was 1 mm, where (a) and (c) at the interface, and (b) and (d) at the cladding layer

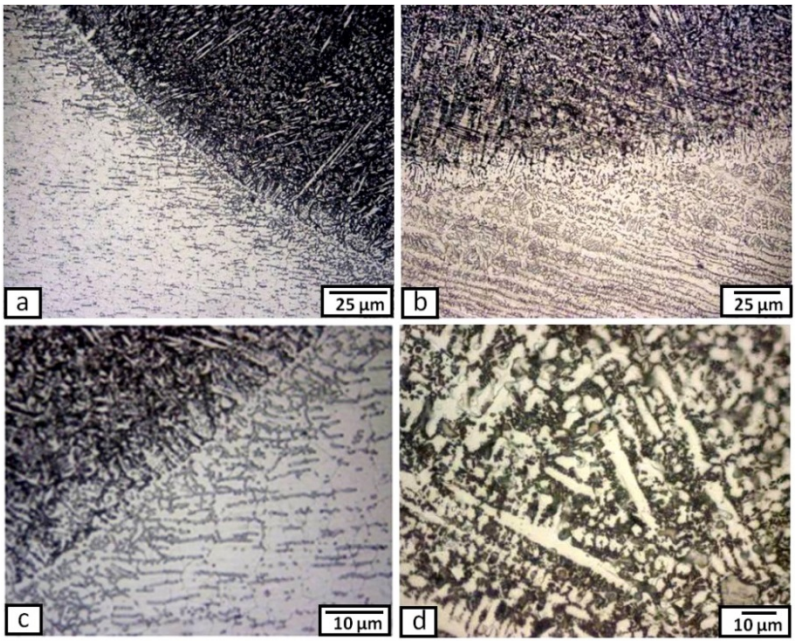

Fig. 6 Micrographs of the different zone at laser treated layer with power of 2800 W and travelling speed of 12 mm/s, when the thickness of preplaced TiC power was 1 mm

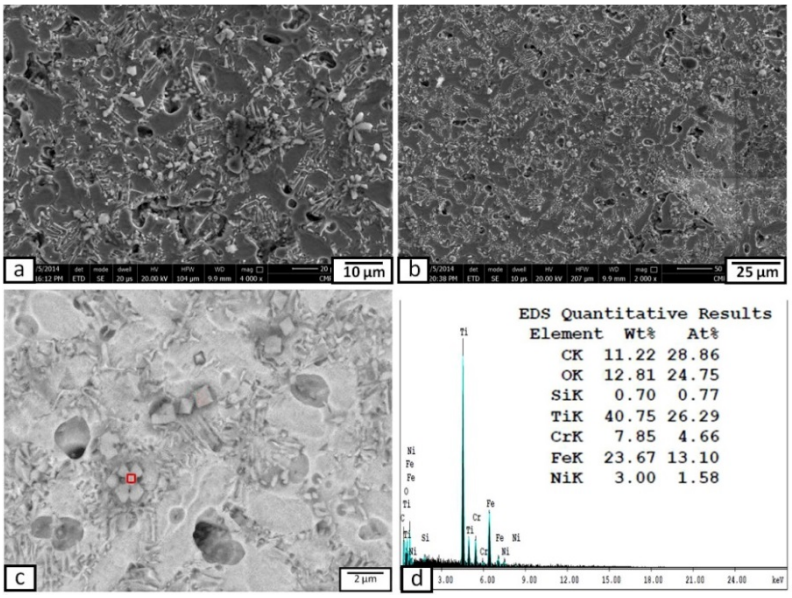

Fig. 7 Micrographs (a - c)of the cladding layer with power of 2800 W and travelling speed of 12 mm/s, when the thickness of preplaced TiC power was 1 mm, and (d) EDX spectra of the elements of red mark in (c)

By increasing the travelling speed to 12 mm/s, the interface between the cladding layer and the substrate stainless steel is adherent, sharp and defect free as shown in Fig 6. The TiC in the cladding layer was distributed homogenously and consisted of fine long dendrites at the top portion and at the lower contour of the cladding layer. This may be due to the relatively fast cooling rate after faster travelling speed. In some areas at the center of the cladding layer, some of the TiC particles appeared as short random oriented dendrites. Moreover, some of these carbides appeared as a rosette shape morphology as shown in Fig. 7.

In severe applications, where the wear is a main failure mode, it is better to increase the thickness of the hard layer deposited on the substrate. For this reason, the thickness of the preplaced TiC powder was increased to be 2 mm. The used processing power and travelling speed were 2800 W and 4 mm/s, respectively. The produced cross-section microstructures were shown in Fig. 8. The cladding layer was consisted of two regions. The TiC powder appeared as

dense clusters of interlocked particles in the upper portion. At these areas, there was almost no stainless steel matrix as shown in Fig. 8(b). The lower portion of the cladding layer was composed of TiC particles with their round shape surrounded by the stainless steel matrix. The heat generated is not enough to melt the thick TiC particles layer. Near the interface, some TiC particles were melted and appeared as dendrites with random orientation or rosette shape as shown in Fig. 9.

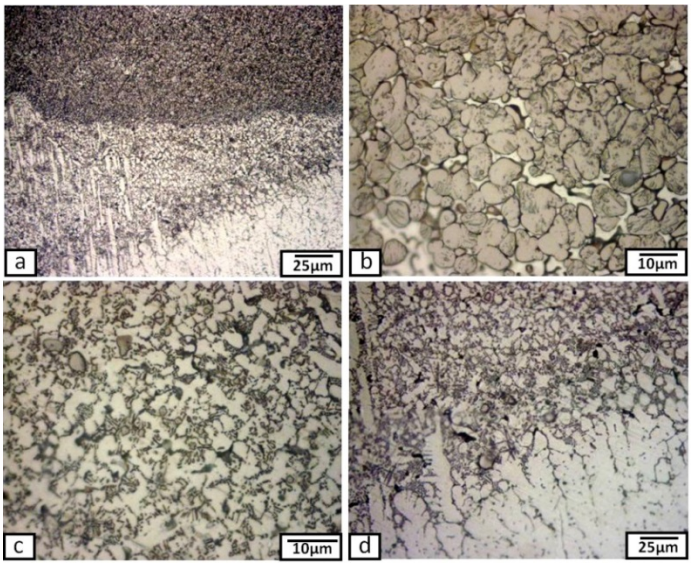

Fig. 8 Micrographs of the different zone at laser treated layer with power of 2800 W and travelling speed of 4 mm/s, when the thickness of preplaced TiC power was 2 mm, where (a) and (d) at the interface, (b) at the top portion of the cladding layer, and (c) at the lower portion of the cladding layer

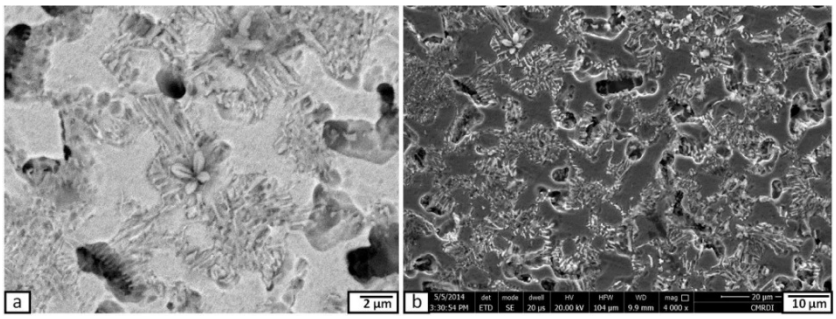

Fig. 9 Micrographs of the cladding layer with power of 2800 W and travelling speed of 4 mm/s, when the thickness of preplaced TiC power was 2 mm

3.2 Surface and subsurface microhardness evaluation

Fig. 10 shows the microhardness distribution through the depth of the laser treated zone obtained at different travelling speeds (4 mm/s, 8 mm/s, 12 mm/s) and preplaced powder thicknesses (1 mm and 2 mm). Generally, the hardness of the cladding layer is much higher (almost three times) than that of the base metal. This is may be due to the hard TiC particles which were distributed homogenously through the cladding layer. The cladding layer which formed with faster travelling speeds show higher hardness that that formed with slower ones. This is due to that the faster travelling speeds yields a finer dendritic TiC, which share in hardness increment. The average hardness values at the surface treated by 12 mm/s travelling speed was about 600 HV.

When the preplaced TiC powder thickness was increased to 2 mm thick, the cladding layer showed ultrahigh hardness values (reached to more than 2000 HV), especially at the top portion of the cladding layer (near the free surface). This is due to the compacted dense hard TiC particles that formed on the top portion of the cladding layer.

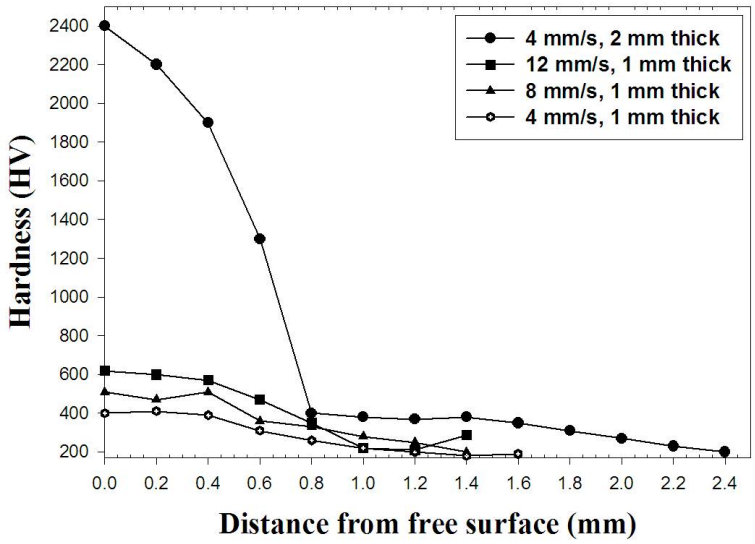

Fig. 10 Microhardness distributions through the laser treated layer cross-sections at different travelling speeds and preplaced powder thicknesses, and fixed power of 2800 W

3.3. Wear and corrosion resistance of the developed surface layer

Fig. 11 shows the variation of wear weight losses of the laser cladding layers using different laser travelling speeds (4 mm/s, 8 mm/s, 12 mm/s) and preplaced powder thicknesses (1 mm and 2 mm) together with the substrate, after subjected to pin-on-disk dry sliding wear test at a fixed load of 2 kg in air at room temperatures. Compared with the substrate, the wear resistance of the laser cladding layer was improved by at least three times. The wear rate was decreased by increasing the travelling speed. This is may be due to the higher hardness achieved at these speeds. On the other hand, the sample that had a preplaced TiC powder of 2 mm, showed exceptional wear resistance (the wear rate was very small, about 0.02 g). This improvement in wear resistance came from the hard, wear resistant, and dense TiC particles which formed at this condition.

Regarding the corrosion resistance evaluation, the sample cladded at travelling speed of 12 mm/s and processing power of 2800 W was chosen due to that it gave the best results regarding the microstructure, hardness and wear resistance. Fig. 12 shows the polarization curves of stainless steel substrate and the cladding layer. The different two branches in each plots represents the anodic (dark one) and cathodic polarization curves. It represents the nature of the reaction at the corrosion potential, e.g., whether the metal is active, passive or active/passive in the corrosion environment. It is well known that when the potential is increased and the current is decreased, the polarization resistance is increased and the material show improved corrosion resistance. From this figure, it is clear that the corrosion current of the cladded layer showed lower values than that of the stainless steel substrate. Also, the corrosion potential of the cladded sample was shifted to more positive than that of the stainless steel substrate. Based on this, the laser cladding of TiC particles on the 304 stainless steel substrate had a positive influence on the corrosion behavior of the coatings. This can be related to the grain refinement of the matrix by the influence of the fast cooling after laser processing. Also, to the good metallurgical bonds of the TiC particles/dendrites with the matrix which give higher chemical stability of the coating. Moreover, the TiC reinforcement acts as obstacles for pitting.

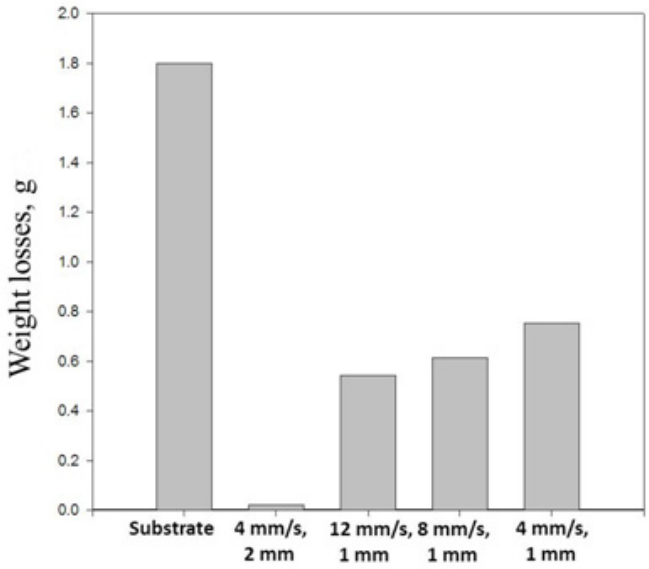

Fig. 11 Wear weight losses of the substrate and specimens treated at different travelling speeds (4 mm/s, 8 mm/s, 12 mm/s) and preplaced powder thicknesses (1 mm and 2 mm), and fixed power of 2800 W

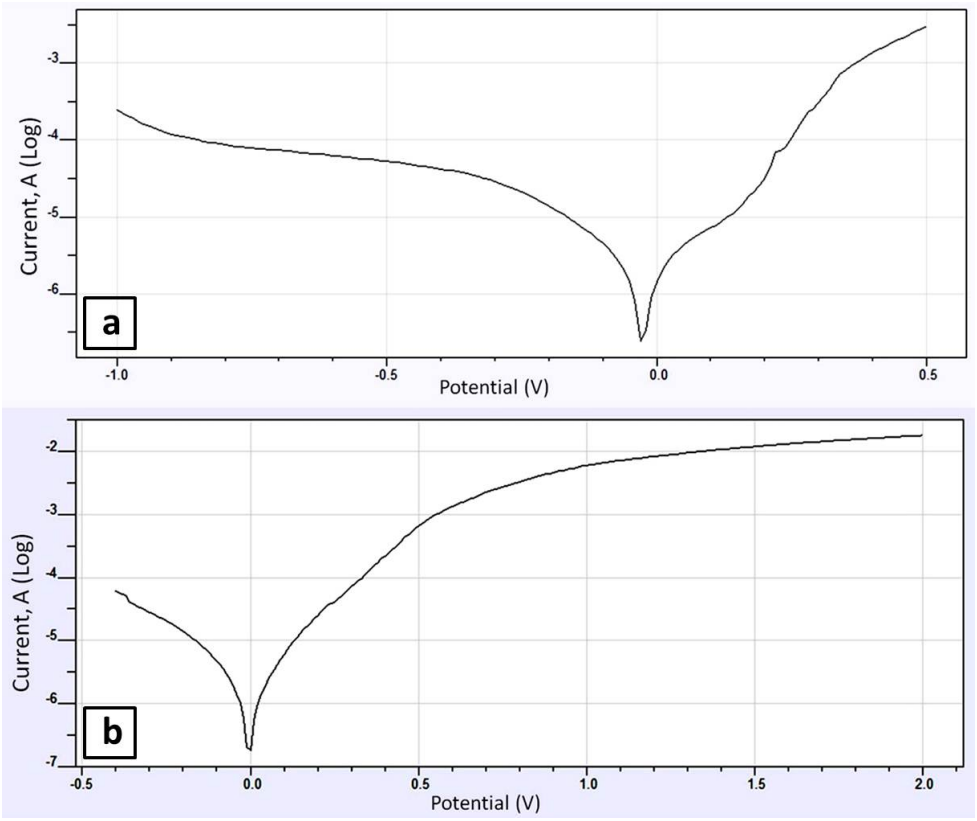

Fig. 12 Polarization curves of the substrate (a), and the cladding layer produced with travelling speed of 12 mm/s and processing power of 2800 W

4. Conclusion

304 stainless steel specimens were YAG fiber laser cladded with TiC powder using processing power of 2800 W and travelling speeds of 4 mm/s, 8 mm/s, and 12 mm/s. The TiC powder with a particle size of 3-10 μm were preplaced on the cleaned surface to form a layer of two different thicknesses: 1 mm and 2 mm. The microstructures of the coated layers and substrate were investigated. The micro-Vickers hardness was measured through the depth of the coated layers cross-section. The wear behaviour of the laser cladded layers was evaluated. The corrosion behavior of the substrate and the cladding layer were evaluated by the corrosion current density and the corrosion potential obtained from polarization curves in a 3.5 wt. % NaCl solution at room temperature. The results of this study lead to the following conclusions:

- Metal matrix composite reinforced with TiC particles was produced in the cladded layer on 304 stainless steel specimens by application of laser cladding treatment at all processing conditions.
- Some of the TiC particles were melted and re-solidified as dendrites during the cladding processing. The amount of the dendritic TiC structure was increased by increasing of the travelling speed.
- The cladding layer produced with higher travelling speed (12 mm/s) was tightly bonded with the substrate without any cracks or any other defects, while that produced at travelling speed of 4 mm/s showed some cracks and crack-networked at the interface and the heat affected zone.
- The TiC particles were clustered in the top portion of the cladding layer when the preplaced powder was 2 mm.
- The hardness of the cladding layer was improved at all processing conditions to be three times at 12 mm/s travelling speed. When the preplaced TiC power was increased to 2 mm, the hardness showed ultrahigh values (more than 2000 HV).
- The wear resistance of the cladding layers was remarkably improved especially at higher travelling speed.
- The corrosion resistance of the cladding layer produced by travelling speed of 12 mm/s was better than that of the stainless steel substrate.

References

[1] Xu, P., Lin, C.X., Zhou, C.Y., Yi, X.P. (2013). Wear and corrosion resistance of laser cladding AISI 304 stainless steel/Al_2O_3 composite coatings, *Surface and Coatings Technology*, Vol. 238, 9-14, doi: 10.1016/j.surfcoat.2013.10.028.

[2] Ul-Hamid, A., Tawancy, H.M., Abbas, N.M. (2012). Failure of weld joints between carbon steel pipe and 304 stainless steel elbows, *Engineering Failure Analysis*, Vol. 12, No. 2, 181-191, doi: 10.1016/j.engfailanal.2004.07.003.

[3] Fissolo, A., Stelmaszyk, J.M., Gourdin, C., Bouin, P., Pérez, G. (2010). Thermal fatigue loading for a type 304-L stainless steel used for pressure water reactor: Investigations on the effect of a nearly perfect biaxial loading, and on the cumulative fatigue life, *Procedia Engineering*, Vol. 2, No. 1, 1595-604, doi: 10.1016/j.proeng.2010.03.172.

[4] Chiu, K.Y., Cheng, F.T., Man, H.C. (2005). Laser cladding of austenitic stainless steel using NiTi strips for resisting cavitation erosion, *Materials Science and Engineering: A*, Vol. 402, No. 1-2, 126-134, doi: 10.1016/j.msea.2005.04.013.

[5] Majumdar, J.D., Chandra, B.R., Manna, I. (2007). Laser composite surfacing of AISI 304 stainless steel with titanium boride for improved wear resistance, *Tribology International*, Vol. 40, No. 1, 146-152, doi: 10.1016/j.triboint.2006.04.006.

[6] Li, S.C. (2000). Cavitation damage in turbines, In: Li, S.C. (ed.), *Cavitation of Hydraulic Machinery*, Imperial College Press, 277-294.

[7] Yang, Y.L., Guo, N., Li, J.F. (2013). Synthesizing, microstructure and microhardness distribution of Ti–Si–C–N/TiCN composite coating on Ti–6Al–4V by laser cladding, *Surface and Coatings Technology*, Vol. 219, 1-7, doi: 10.1016/j.surfcoat.2012.12.038.

[8] Qiu, X.W., Zhang, Y.P., He, L., Liu, C.G. (2013). Microstructure and corrosion resistance of AlCrFeCuCo high entropy alloy, *Journal of Alloys and Compounds*, Vol. 549, 195-199, doi: 10.1016/j.jallcom.2012.09.091.

[9] Guo, C., Zhou, J.S., Chen, J.M., Zhao, J.R., Yu, Y.J., Zhou, H.D. (2010). Improvement of the oxidation and wear resistance of pure Ti by laser cladding at elevated temperature, *Surface and Coatings Technology*, Vol. 205, No. 7, 2142-2151, doi: 10.1016/j.surfcoat.2010.08.125.
[10] Thawari, G., Sundararajan, G., Joshi, S.V. (2003). Laser surface alloying of medium carbon steel with $SiC_{(P)}$, *Thin Solid Films*, Vol. 423, No. 1, 41-53, doi: 10.1016/S0040-6090(02)00974-4.
[11] Liang, G.Y., Wong, T.T., MacAlpine, J.M.K., Su. J.Y. (2000). Study of wear resistance of plasma-sprayed and laser-remelted coatings on aluminium alloy, *Surface and Coatings Technology*, Vol. 127, No. 2-3, 232-237, doi: 10.1016/s0257-8972(00)00551-x.
[12] Sun, R.L., Yang, D.Z., Guo, L.X., Dong, S.L. (2001). Laser cladding of Ti–6Al–4V alloy with TiC and TiC+NiCrBSi powders, *Surface and Coatings Technology*, Vol. 135, No. 2-3, 307-312, doi: 10.1016/S0257-8972(00)01082-3.
[13] Sun, R.L., Mao, J.F., Yang, D.Z. (2002). Microscopic morphology and distribution of TiC phase in laser clad NiCrBSiC–TiC layer on titanium alloy substrate, *Surface and Coatings Technology*, Vol. 155, No. 2-3, 203-207, doi: 10.1016/S0257-8972(02)00006-3.
[14] Mateos, J., Cuetos, J.M., Fernández, E., Vijande, R. (2000). Tribological behaviour of plasma-sprayed WC coatings with and without laser remelting, *Wear*, Vol. 239, No. 2, 274-281, doi: 10.1016/S0043-1648(00)00325-2.
[15] Cheng, F.T., Kwok, C.T., Man, H.C. (2001). Laser surfacing of S31603 stainless steel with engineering ceramics for cavitation erosion resistance, *Surface and Coatings Technology*, Vol. 139, No. 1, 14-24, doi: 10.1016/S0257-8972(00)01103-8.
[16] Mahmoud, E.R.I., El-Labban, H.F. (2014). Laser surface cladding of high C-Cr bearing tool steel with TiC powders, *The IUP Journal of Mechanical Engineering*, Vol. 7, No. 4, 67-79.
[17] Liu, Y.F., Mu, J.S., Xu, X.Y., Yang, S.Z. (2007). Microstructure and dry-sliding wear properties of TiC-reinforced composite coating prepared by plasma-transferred arc weld-surfacing process, *Materials Science and Engineering: A*, Vol. 458, No. 1-2, 366-370, doi: 10.1016/j.msea.2006.12.086.
[18] Dong, Y.J., Wang, H.M. (2009). Microstructure and dry sliding wear resistance of laser clad TiC reinforced Ti–Ni–Si intermetallic composite coating, *Surface and Coatings Technology*, Vol. 204, No. 5, 731-735, doi: 10.1016/j.surfcoat.2009.09.024.
[19] Deng, J.X., Liu, L., Yang, X.F., Liu, J.H., Sun, J.L., Zhao, J.L. (2007). Self-lubrication of Al_2O_3/TiC/CaF_2 ceramic composites in sliding wear tests and in machining processes, *Materials & Design*, Vol. 28, No. 3, 757-764, doi: 10.1016/j.matdes. 2005.12.003.
[20] Moya, J.S., Lopez-Esteban, S., Pecharromán, C. (2007). The challenge of ceramic/metal microcomposites and nanocomposites, *Progress in Materials Science*, Vol. 52, No. 7, 1017-1090, doi: 10.1016/j.pmatsci.2006.09.003.
[21] Lo, K.H., Cheng, F.T., Man, H.C. (2003). Cavitation erosion mechanism of S31600 stainless steel laser surface-modified with unclad WC, *Materials Science and Engineering: A*, Vol. 357, No. 1-2, 168-180, doi: 10.1016/S0921-5093(03)00216-8.
[22] Laroudie, F., Tassin, C., Pons, M. (1995). Hardening of 316L stainless steel by laser surface alloying, *Journal of Materials Science*, Vol. 30, No. 14, 3652-3657, doi: 10.1007/BF00351880.
[23] Guan, K., Wang, Z., Gao, M., Li, X., Zeng, X. (2013). Effects of processing parameters on tensile properties of selective laser melted 304 stainless steel, *Materials & Design*, Vol. 50, 581-586, doi: 10.1016/j.matdes. 2013.03.056.
[24] Viswanathan, A., Sastikumar, D., Rajarajan, P., Kumar, H., Nath, A.K. (2007). Laser irradiation of AISI 316L stainless steel coated with Si_3N_4 and Ti, *Optics & Laser Technology*, Vol. 39, No. 8, 1504-1513, doi: 10.1016/j.optlastec. 2007.01.004.
[25] Zhang, D., Zhang, X. (2005). Laser cladding of stainless steel with Ni-Cr_3C_2 and Ni-WC for improving erosive-corrosive wear performance, *Surface and Coatings Technology*, Vol. 190, No. 2-3, 212-217, doi: 10.1016/j.surfcoat. 2004.03.018.
[26] Majumdar, J.D., Manna, I. (1999). Laser surface alloying of AISI304-stainless steel with molybdenum for improvement in pitting and erosion-corrosion resistance, *Materials Science and Engineering: A*, Vol. 267, No. 1, 50-59, doi: 10.1016/S0921-5093(99)00053-2.
[27] El-Labban, H.F., Mahmoud, E.R.I., Al-Wadai, H. (2014). Laser cladding of Ti-6Al-4V alloy with vanadium carbide particles, *Advances in Production Engineering & Management*, Vol. 9, No. 4, 159-167, doi: 10.14743/apem 2014.4.184.